J Mater Sci (2007) 42:6382–6387
DOI 10.1007/s10853-006-1205-2

MD simulations on the melting and compression of C, SiC and Si nanotubes

Haijun Shen

Received: 9 June 2006 / Accepted: 2 November 2006 / Published online: 27 April 2007

Abstract By the Tersoff potential based molecular dynamics (MD) method, the melting and axial compression of the (5,5) C, SiC, and Si nanotubes are simulated, and their molecular configurations, atomic radial distribution functions (RDF) and energy changes during heating-up, as well as their compressive force–strain curves, are obtained. According to the computed results, the differences of the melting and compressive mechanical properties of the three nanotubes are discussed. It is found that the melting C, SiC, and Si nanotubes have netlike, loose spherical and compact spherical configurations respectively, and that the C nanotube has the highest melting point, specific heat, melting heat and load support capability, whereas the Si nanotube has the lowest ones.

Introduction

Since discovered by Ijima in the early 1990s [1], single-walled carbon nanotubes (SWCNTs) have become attractive new materials with many important potential applications [2, 3]. Due to the fact that silicon and carbon lie in the same group of the element periodic table and have the similar electronic structure, people hope to be able to find the single-walled silicon nanotubes similar to SWCNTs sometime [4, 5]. Recently Tang et al. [6] obtained hollow Si nanotubes under supercritically hydrothermal conditions, but their Si nanotubes were found to have just the walls of diamond-like structure. Even if the single-walled silicon nanotubes, i.e., the Si nanotubes with single-layer graphite-like walls, have never been observed up to now, many correlative theoretical predictions have still been performed in recent years [4, 5, 7–9]. In most of the work, the Quantum mechanics (QM) methods, such as density function theory (DFT) and ab initio, were used, and the attentions were mainly paid on the micro-structural and electronic properties of the nanotubes. The work has implied the possibility of the Si nanotubes with single-layer graphite-like walls.

Silicon is the important material of microelectronic devices, whereas carbon is the potential element to replace Si in future nano-electromechanical systems (NEMS). Obviously, it is very necessary to systematically investigate the various properties of C and Si nanotubes. Now the studies on the thermodynamic and mechanical characters of carbon nanotubes have been carried out [3, 10–12], but the correlative work on single-walled Si nanotubes is little reported. Considering the reason, in the present paper the Tersoff potential based molecular dynamics (MD) simulations are performed to investigate the melting and compression of the (5,5) C, SiC, and Si nanotubes, and further the simulated results are used to analyze the differences of their melting and compressive properties.

Model

The investigated objects

In this paper three armchair (5,5) nanotubes of C, SiC, and Si are chosen as objects to be investigated, see Fig. 1. The model of the (5,5) C nanotube is gotten through the nanotube-generator [10], a software developed by us. According to the configurations of the SiC and Si

H. Shen (✉)
School of Aeronautics and Astronautics, Nanjing University of Aeronautics & Astronautics, Nanjing 210016, China
e-mail: shj@nuaa.edu.cn

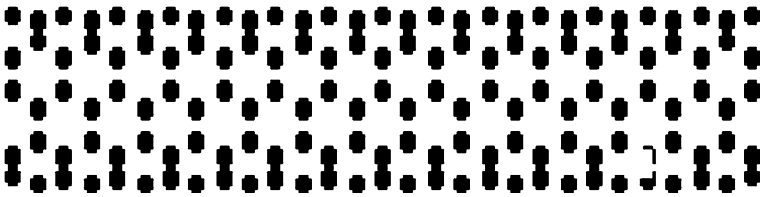

Fig. 1 The single-walled C, SiC, or Si nanotube

nanotubes given in Refs. [13] and [9], respectively, the (5,5) SiC and Si nanotubes are ''constructed'' by replacing the carbon atoms of the (5,5) C tube with silicon atoms at intervals or completely. All the three nanotubes have 290 atoms and the single-layer graphite-like walls. After the nanotubes are geometrically optimized, we will get their initial molecular configurations. Here the geometrical optimization is carried out by molecular mechanics method in the quantum-chemical software of HyperChem 7®. In the optimization, the MM+ force-field, the conjugate gradient method by Fletcher et al. [14], and the convergence limit of 0.01 Kcal/mol are taken. The optimized C, SiC, and Si nanotubes have the length of 3.5, 4.3, and 5.2 nm, and the diameter of 0.66, 0.85, and 0.98 nm, respectively. The C–C, C–Si and Si–Si bonds in the C, SiC, and Si nanotubes are about 0.14,0.19, and 0.23 nm long respectively.

Simulation details

MD is a widely used computer simulation technique in condensed matter physics, as well as other disciplines ranging from chemistry to high-energy physics. In MD, the time evolution of interacting atoms is followed by integrating their equations of motion, which can help people to comprehend more details of matter motion at atomic level. Generally speaking, many-body potentials can more accurately describe the interactions between atoms than simple pair-potentials. Of the available many-body potentials, Tersoff potential, a famous bond order potential derived from quantum-mechanical arguments, can well consider bond order and covalent bonds forming/breaking [15–18] and has been widely used to calculate the lattice constants, bulk modulus and cohesive energy of diamond, graphite, carbon nanotube and Si semiconductor material. So the Tersoff potential is adopted to simulate the melting and compression of the C, SiC, and Si nanotubes here.

For the interactions between two neighbouring atoms i and j, the form of the energy Φ is taken to be [16]

$$\Phi = \sum_i \sum_{j>i} f_c[a_{ij} \cdot E_r(r_{ij}) - b_{ij} \cdot E_a(r_{ij})] \tag{1}$$

with

$$\begin{aligned} E_r(r_{ij}) &= A_{ij} \cdot \exp(-\lambda_{ij} \cdot r_{ij}) \\ E_a(r_{ij}) &= B_{ij} \cdot \exp(-\mu_{ij} \cdot r_{ij}) \\ f_c(r_{ij}) &= \begin{cases} 1 & r_{ij} < R_{ij} \\ \frac{1}{2}\left[1 + \cos\left(\pi \frac{r_{ij}-R_{ij}}{S_{ij}-R_{ij}}\right)\right] & R_{ij} < r_{ij} < S_{ij} \\ 0 & S_{ij} < r_{ij} \end{cases} \end{aligned} \tag{2}$$

b_{ij} is the many-body order parameter describing how the bond-formation energy is affected by the local atomic arrangement due to the presence of other neighbouring atoms (the k-atoms). It is a many-body function of the positions of the atoms i, j, and k. It has the form of

$$b_{ij} = \chi_{ij}\left(1 + \beta_i^{n_i} \cdot \xi_{ij}^{n_i}\right)^{-\frac{m_i}{2n_i}} \tag{3}$$

with

$$\begin{aligned} \xi_{ij} &= \sum_{k \neq i,j} f_c(r_{ik}) \omega_{ik} \cdot g(\theta_{ijk}) \\ g(\theta_{ijk}) &= 1 + \frac{c_i^2}{d_i^2} - \frac{c_i^2}{d_i^2 + (h_i + \cos\theta_{ijk})^2} \\ a_{ij} &= \varepsilon_{ij}\left(1 + \beta_i^{n_i} \cdot \tau_{ij}^{n_i}\right)^{\frac{-1}{2n_i}} \\ \tau_{ij} &= \sum_{k \neq i,j} f_c(r_{ij}) \delta_{ik} \cdot g(\theta_{ijk}) \end{aligned}$$

$$\lambda_{ij} = \frac{\lambda_i + \lambda_j}{2} \tag{4}$$

$$\mu_{ij} = \frac{\mu_i + \mu_j}{2} \tag{5}$$

$$A_{ij} = \sqrt{A_i A_j} \tag{6}$$

$$B_{ij} = \sqrt{B_i B_j} \tag{7}$$

where, r_{ij} is the distance of the ith and jth atom, θ_{ijk} is the angle between r_{ij} and r_{jk}, $f_c(r_{ij})$ is a truncation function. A_i, B_i, λ_i, μ_i, ε_{ij}, χ_{ij}, β_i, n_i, m_i, δ_{ik}, ω_{ik}, c_i, d_i, h_i, R_{ij}, and S_{ij} are some correlative constants with the C, C-Si or Si system, and their values take the corresponding ones in Refs. [15–17].

In this paper, the Verlet technique [19] is used to integrate the equations of motion over time steps of $\Delta t = 0.001ps$. The periodic boundary conditions are adopted. The following method, i.e. the method of Ref. [20], is adopted to simulate the melting of the C, SiC, and Si

nanotubes: 1 equilibrating the C, SiC, and Si nanotubes for 50,000Δt at the initial temperature of 2,000 K; 2 increasing the temperature of the molecular systems by 250 K and equilibrating them at the constant temperature for 50,000Δt; 3 repeating Step 2, i.e. ''heating up'', until the nanotubes ''melt''. The following scheme is taken to simulate the axial compression of the C, SiC, and Si nanotubes: fixing the 14 atoms at the left end of the nanotubes, see Fig. 1, and horizontally imposing compressive load on the 14 atoms at the right end in displacement-steps of 0.05 nm per 20,000Δt, where the temperature takes 300 K and is controlled by using the Nose technique [21].

Results and discussion

The melting properties of the C, SiC, and Si nanotubes

Figures 2–4 present the configuration evolvement of the C, SiC, and Si nanotubes during heating up, respectively. Figures 5 and 6 show their RDFs (radial distribution functions) at different temperature and their energy changes with temperature, respectively.

From Fig. 2–4, it is shown that the C, SiC, and Si nanotubes obviously change in configuration after 6250, 4500, and 2750 K, respectively, i.e. they melt. However, their melting processes are evidently different. Among the three nanotubes, when the C nanotube melts, its wall breaks and becomes netlike, and simultaneously a few of C atoms and short C atomic-chains escape from the netlike main-body; when the SiC nanotube melts, it shrinks into one loose sphere first, and with the further increase of temperature some C (or Si) atoms and short C (or Si) atomic-chains give off from the spherical cluster; when the Si nanotube melts, it curls and forms one compact sphere first, the compact cluster holds in configuration with the increase of temperature, and no atom or atomic-chain is observed to escape from the cluster until the temperature of 3250 K.

The RDFs of Fig. 5 can supply further details about the melting of the nanotubes. From Fig. 5, it can be found that:

(1) At low temperature all the RDFs of three nanotubes have sharp peaks. For the C nanotube the first and second peaks are located at 0.14 and 025 nm, for the SiC tube they are at 0.19 and 0.32 nm, and for the Si tube they are at 0.23 and 0.40 nm. These values just correspond to the distances of the adjacent and subadjacent atoms on the walls of the C, SiC, and Si tubes, respectively, which implies that three nanotubes basically hold their own initial configurations.

(2) With the further increase of temperature, all the peaks become lower and wider. Especially after the C, SiC, and Si nanotubes melt at 6250, 4500, and 2750 K, respectively, their RDF curves change prominently. For the C nanotube, the first and second peaks become lower and wider, the third peak has disappeared, but the location of the first and second peaks has no change, which indicates that most of the C atoms remain in the broken graphite-like net just as shown in Fig. 2c, d; for the SiC nanotube, almost all peaks including the first and second peaks disappear, which implies that the atoms of the melting SiC nanotube are highly disorderly; for the Si nanotube, the second peak has disappeared, and the first peak become lower and wider with its location moving from 0.23 to 0.26 nm, where the 0.26 nm is close to the Si–Si bond length (0.255 nm) of single crystal silicon (SCS), which implies that the atoms of the melting Si nanotube are of long-range confusion but have the tetrahedronal configurations of SCS at short-range.

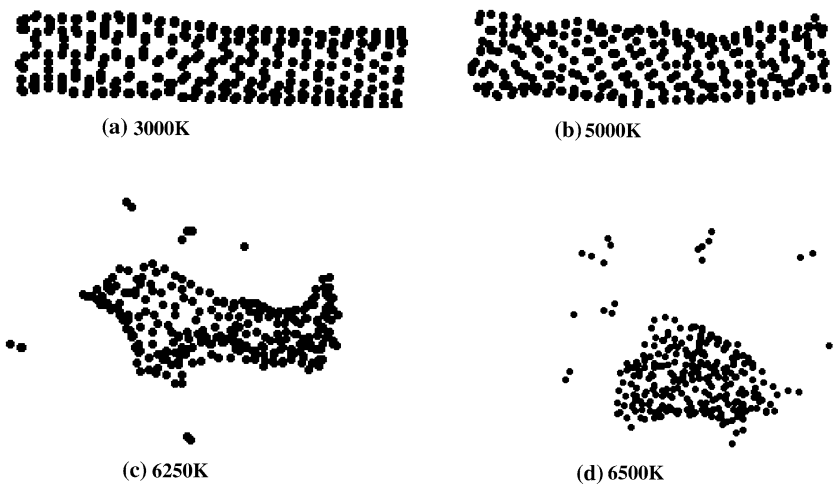

Fig. 2 Melting of the C nanotube. (**a**) 3,000 K; (**b**) 5,000 K; (**c**) 6250 K; and (**d**) 6,500 K

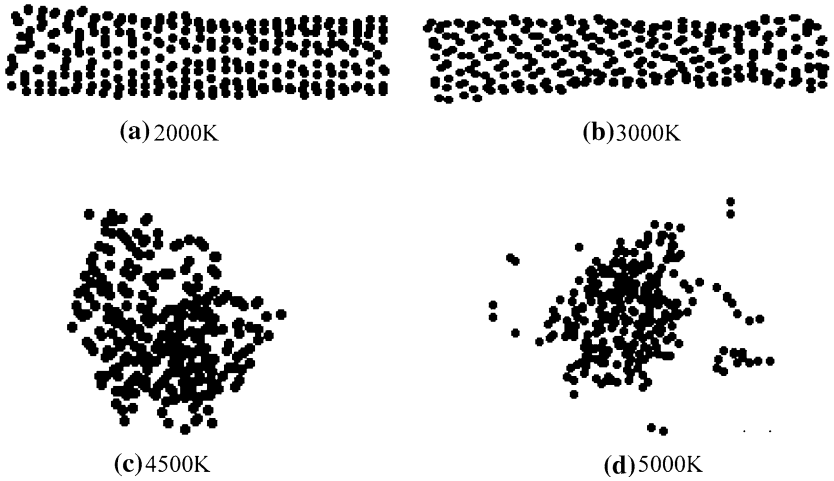

Fig. 3 Melting of the SiC nanotube. (**a**) 2,000 K; (**b**) 3,000 K; (**c**) 4,500 K; and (**d**) 5,000 K

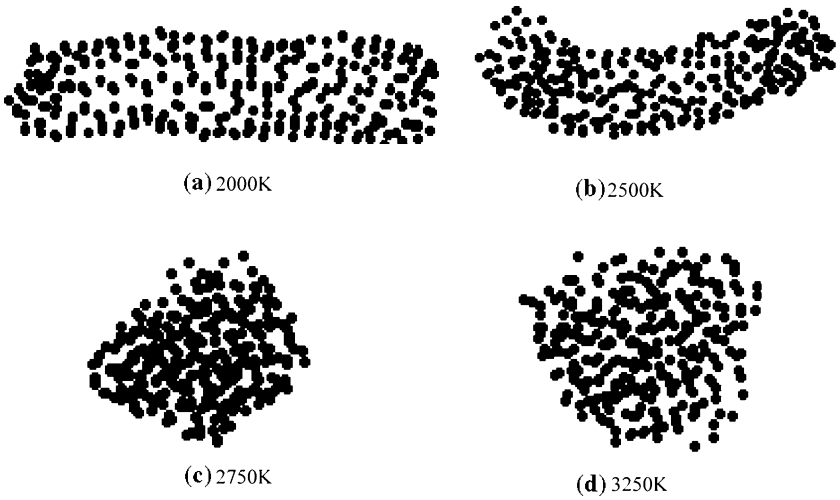

Fig. 4 Melting of the Si nanotube. (**a**) 2,000 K; (**b**) 2,500 K; (**c**) 2,750 K; and (**d**) 3,250 K

From Fig. 6 it is shown that:

(1) With the increase of temperature, the energy of the C, SiC, and Si nanotubes increases, and three discontinuities appear on their own energy-temperature curves at 6,300, 5,600, and 2,250 K, respectively, see the arrowheads ''↑'' marked in Fig. 6. Before and after the discontinuities the curves are approximately linear. Obviously they all are typical crystal melting curves. According to Figs. 2–5, i.e., the configuration evolvement and RDF curves of three nanotubes, it can be inferred that after the discontinuities three nanotubes have big change in configuration, i.e. they have melted.

(2) At the same temperature, the Si nanotube has much higher energy than the C and SiC nanotubes, and the C nanotube has the lowest one. This implies that the Si nanotube has the worst stability and the C nanotube has the best one.

In addition, according to the location of the discontinuities, the height of the discontinuities and the slope of the energy-temperature curves before the discontinuities, we can estimate the melting point, specific heat and melting heat of three nanotubes. The estimated melting point, specific heat and melting heat are listed in Table 1. Note: the specific heat and melting heat in Table 1 are the average ones per atom. Table 1 shows that the melting point, specific heat and melting heat have the same order of ''C > SiC > Si nanotube''. The melting point of the C nanotube is 6,300 K and the specific heat 3.22 K_B. The values are compatible to the melting point (> 4,000 K) and specific heat 3.1 K_B for the C_{60} fullerene in Ref. [20], which indirectly verifies the present MD simulations. Here the K_B is the Boltzmann constant.

In order to consider the effect of tube length on melting properties, the similar MD simulations are also carried out for two other (5,5) carbon-tubes with the

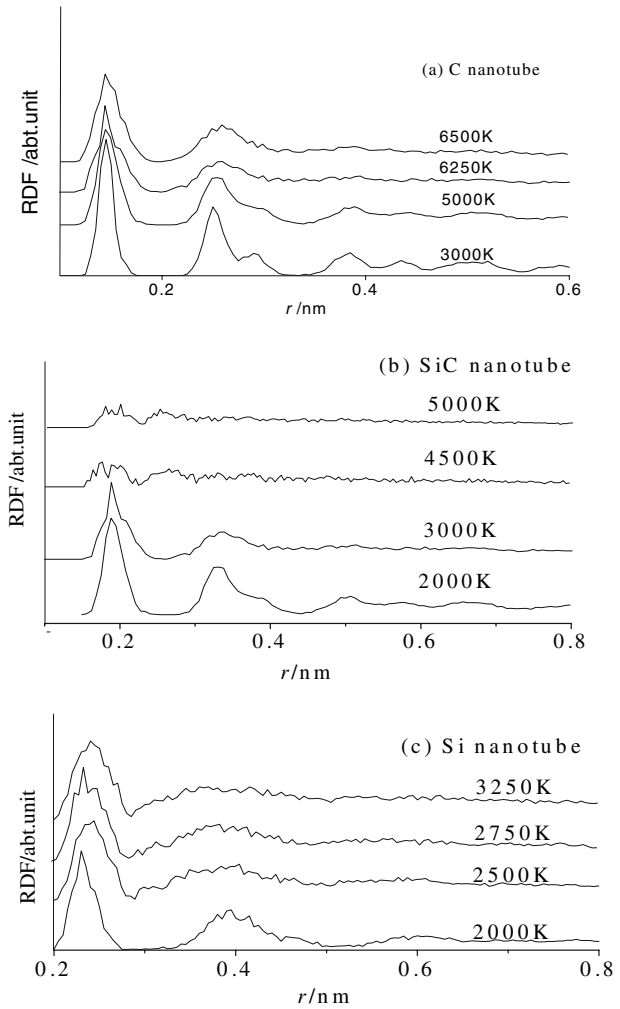

Fig. 5 The radial distribution of nanotubes. (**a**) C nanotube; (**b**) SiC nanotube; and (**c**) Si nanotube

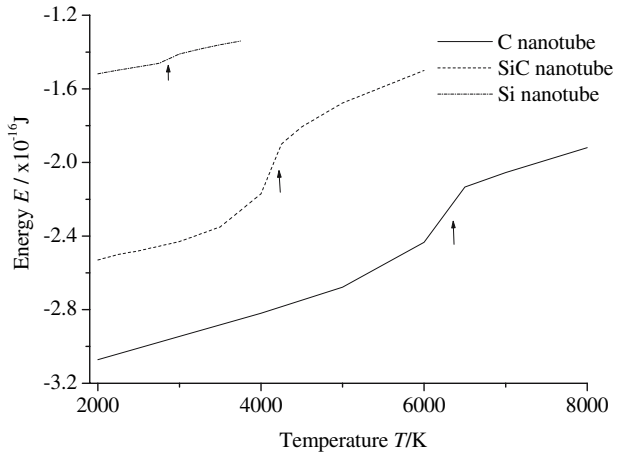

Fig. 6 The energy changes of the C, SiC, and Si nanotubes with temperature

length of 5.2 and 7.1 nm, respectively. The simulated results show that the two (5,5) carbon-tubes have the similar melting process to the case of Fig. 2, their melting point is 6250 and 6400 K, and the specific heat is 3.31 and 3.15 K_B, respectively. By comparing the data with the corresponding ones of the (5,5) carbon-tube in Table 1, it can be found that the melting parameters of the three carbon tubes are very close, and the tube length seems to have only little effect on the melting properties of nanotubes.

The compressive properties of the C, SiC, and Si nanotubes

Figure 7 shows the compressive deformation of the C nanotube. The deformation of the SiC and Si nanotubes under compression is similar to the case of the C nanotube and is not given here. Figure 8 presents the compressive force-strain curves of three nanotubes. In the figure the arrowheads '' ← '' mark the moment of the nanotubes locally buckling on tube-walls, i.e., the moment of their instability.

From Figs. 7 and 8, it can be found that:

(1) With the increase of the compressive strain, the external force of three nanotubes increases; at the moment of their instability, the force reaches maximum; after this, the force of three nanotubes decreases with the increase of strain.

(2) At the same compressive strain, the C nanotube has much higher external-force than the SiC and Si nanotubes, and the Si nanotube has the lowest one. The maximal force of the C, SiC, and Si nanotubes are 56, 21, and 15 nN, and the strain corresponding to the maximal force is 0.101, 0.090, and 0.081, respectively. Here the strain is called as ''failure strain''. The values of the maximal force and failure strain are also listed in Table 1. The maximal force and failure strain are often used to characterize the load and deformation support capability of materials [22]. Generally speaking, the materials with higher maximal force and failure strain have better load and deformation support capability. Obviously, the C nanotube has the best load and deformation support capability, whereas the Si tube has the worst ones.

(3) In Ref. [23] the MD method is used to simulate the axial compression of one (5,5) C nanotube, and the calculated maximal compressive loading is 49 nN. The result is close to the present one 56 nN, which further verifies our MD simulations.

Table 1 The melting and compressive parameters of the C, SiC, and Si nanotubes

	Melting point /K	Specific heat K_B	Melting heat / $\times 10^{-20}$ J	Failure strain	Maximal load /nN
C tube	6,300	3.22	9.55	0.101	56
SiC tube	5,800	3.19	8.83	0.090	21
Si tube	2,250	1.75	1.79	0.081	15

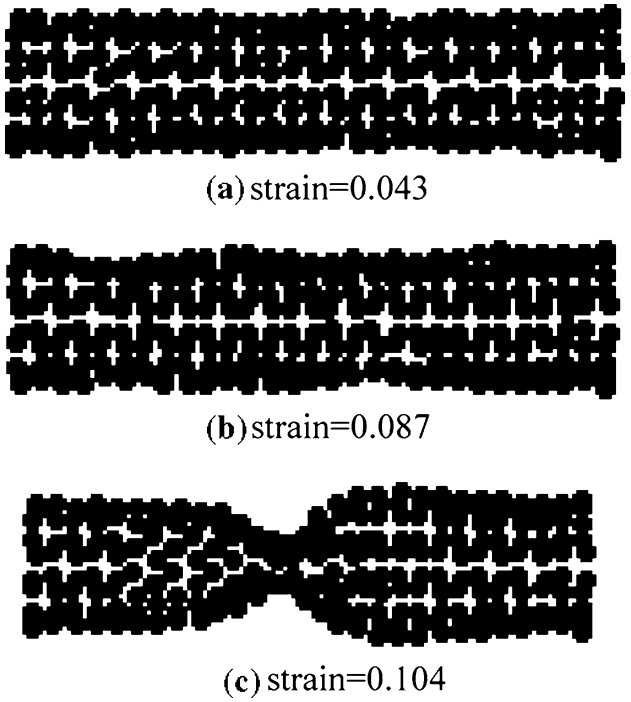

Fig. 7 The compressive deformation of the C nanotube (**a**) strain = 0.043; (**b**) strain = 0.087; and (**c**) strain = 0.104

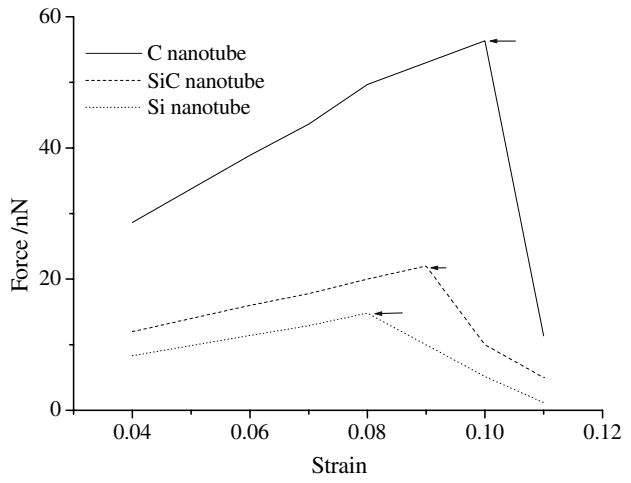

Fig. 8 The force-strain curves of three nanotubes

Conclusions

In the present paper, the classical MD method is used to simulate the melting and compression of the (5,5) C, SiC, and Si nanotubes, and their geometrical configurations, atomic radial distribution functions and energy changes during ''heating up'', as well as their compressive force-strain curves, are obtained. Further, according to the simulated results, the melting and compressive properties of three nanotubes are compared and analyzed. The results show that the melting C, SiC, and Si nanotubes have the netlike, loose spherical and compact spherical configuration, respectively, that their melting points are about 6300, 5600, and 2250 K, respectively, and that the C nanotube has the highest melting point, specific heat, melting heat and load support capability, whereas the Si nanotube has the lowest ones.

Acknowledgement The paper is supported by the NUAA Innovation Fund.

References

1. Iijima SH (1991) Nature 354(6348):56
2. Dai HJ, Hafner JH, Rinzler AG, Colbert DT, Smalley RE (1996) Nature 384(6605):147
3. Shen H, Mu X (2005) J Mater Sci Eng 23(3):321
4. Dmitrii FP, Federico R (2006) Small 2(1):22
5. Seifert G, Köhler Th, Urbassek HM, Hernández E, Frauenheim Th (2001) Phys Rev B 63:193409
6. Tang YH, Pei LZ, Chen YW, Guo C (2005) Phys Rev Lett 95:116102
7. Durgun E, Tongay S, Ciraci S (2005) Phys Rev B 72:75420
8. Durgun E, Tongay S, Ciraci S (2005) Turk J Phys 29:307
9. Jaeil B, Zeng XC, Hideki T, Zeng JY (2004) Chemistry 101(9):2664
10. Shen H (2004) Comput Appl Chem 21(3):485
11. Young-Kyun K, Savas B, David T (2004) Phys Rev Lett 92:15901
12. Yeau-Ren J, Ping-Chi T (2005) J Chem Phys 122:224713
13. Madhu M, Ernst R (2004) Phys Rev B 69:115322
14. Fletcher R, Reeves C (1964) Comput J 7:149
15. Tersoff J (1998) Phys Rev Lett 56(6):632
16. Tersoff J (1988) Phys Rev Lett 61:2879
17. Sekkai W, Zaoui A (2002) New J Phys 4:91
18. Tersoff J (1989) Phys Rev B 39(8):5566
19. Leach AR (1996) Molecular modeling. Addison Wesley Longman Limited, pp 316–317
20. Seong GK, David T (1999) Phys Rev Lett 72:2418
21. Nose S (1984) J Chem Phys 81(1):511
22. Shen H (2006) Chinese J Mater Res 20(1):93
23. Wang L, Hu H (2004) Acta Mech Solida Sinica 25(3):233